

08.1

Peculiarities of nucleation and growth of InGaN nanowires on SiC/Si substrates by HVPE

© S.A. Kukushkin^{1,2}, A.V. Osipov^{1,2}, A.V. Redkov^{1,2}, V.M. Stozharov³, E.V. Ubiyovk¹,
Sh.Sh. Sharofidinov⁴

¹ St. Petersburg State University, St. Petersburg, Russia

² Institute for Problems in Mechanical Engineering, Russian Academy of Sciences, St. Petersburg, Russia

³ Scientific and Technical Center New Technologies (STC NT), St. Petersburg, Russia

⁴ Ioffe Institute, St. Petersburg, Russia

E-mail: sergey.a.kukushkin@gmail.com

Received October 20, 2021

Revised October 20, 2021

Accepted November 15, 2021

The growth of InGaN layers on hybrid SiC/Si substrates with orientations (100), (110), and (111) by the HVPE method was studied at temperatures that wittingly exceed the temperature of InN decomposition onto nitrogen atoms and metallic In (1000°C). On substrates with orientations (110) and (111), the formation of InGaN whisker nanocrystals was observed. The shape and growth mechanisms of nanocrystals were investigated. It is shown that nanocrystals nucleate on the (111) surface only inside *V*-defects formed at the points where screw dislocations exit onto the surface. On the (110) surface, nanocrystals are formed only on pedestals that arise during the film growth. An explanation is given for the difference in the growth mechanisms of nanocrystals on substrates of different orientations.

Keywords: InGaN, heterostructures, SiC on Si, silicon, whisker nanocrystals, nanostructures, atomic substitution method

DOI: 10.21883/TPL.2022.02.53584.19056

It is common knowledge that the efficiency of optoelectronic devices operating in the yellow-green optical range and utilizing InGaN heterostructures with a high indium content is very hard to enhance. This is attributable primarily to the complexity of fabrication of low-defect InGaN films. The authors of [1–3] proposed to address this issue by using whisker nanocrystals (WNCs) instead of epitaxial In-containing solid layers in the fabrication of heterostructures, since almost no mismatch dislocations form in nanocrystals themselves [4]. Note that the majority of studies are focused on the growth by molecular-beam epitaxy or metalorganic vapor phase epitaxy. However, it is even harder to grow epitaxial InN layers by hydride vapor phase epitaxy (HVPE) [5–10], since InN decomposes into metallic indium and nitrogen molecules at a near-atmospheric pressure of reaction gases and temperatures exceeding 500°C [8]. It was also found in [11] that In has a significant effect on the rate of growth of AlGaIn films and on their structural characteristics. In view of this, the aim of the present study is to examine the effect of indium on the HVPE growth of GaN films at temperatures well above the InN decomposition temperature. Indium was intended to be used as a kind of catalyst that exerts a short-term influence on the process of GaN nucleation and is then removed from the reaction region.

Experiments were performed on *p*-type (100), (110), and (111) Si substrates. At the first stage, *nano*-SiC/Si layers were synthesized on these substrates in accordance with the method outlined in [12] under the following conditions: $T = 1290^\circ\text{C}$; $P = 0.5$ Torr; SiH_4 and CO fluxes — 12 and

0.25 sccm, respectively; $t = 20$ min. A buffer AlN layer was then deposited by HVPE [13,14] at a temperature of 1000°C within 3 min. At the next stage, a gas mixture of gallium and indium chlorides ($\text{Ga/In} = 80:20$) and HCl was fed for 3 min into the growth chamber. The growth conditions on substrates of all orientations were the same. Following synthesis, the samples were subjected to scanning electron microscopy (Tescan Mira 3 with an energy dispersive spectroscopy (EDS) attachment), Raman spectroscopy (Witec Alpha 300R), and X-ray diffractometry (DRON-8).

It was found that whisker nanocrystals formed on the surfaces of (110) and (111) substrates in the process of GaN growth with the addition of InN (Fig. 1). The formation of whisker nanocrystals has not been observed in [13,14] when GaN was grown under the same conditions without indium. WNCs did not form on the substrate with orientation (100). In addition, a vanishingly small amount of InN was present in the layers on (110) and (111) substrates. EDS measurements and Raman spectroscopy data did not reveal the presence of InN in the layers. InN-containing phases were detected only in X-ray diffractometry studies. Substrates with orientation (100) were free from InN, at least within the sensitivity of instruments used in our experiments. Figure 2 shows an example diffraction pattern of the sample grown on the (111) substrate. Upper-bound estimates of elastic stresses were obtained based the shift of Bragg angles for hexagonal axis *c*: $\sigma_{\text{InN}} \approx -4$ GPa and $\sigma_{\text{GaN}} \approx -12$ GPa. The corresponding values for the (110) substrate were lower: $\sigma_{\text{InN}} \approx -0.78$ GPa and $\sigma_{\text{GaN}} \approx 3$ GPa.

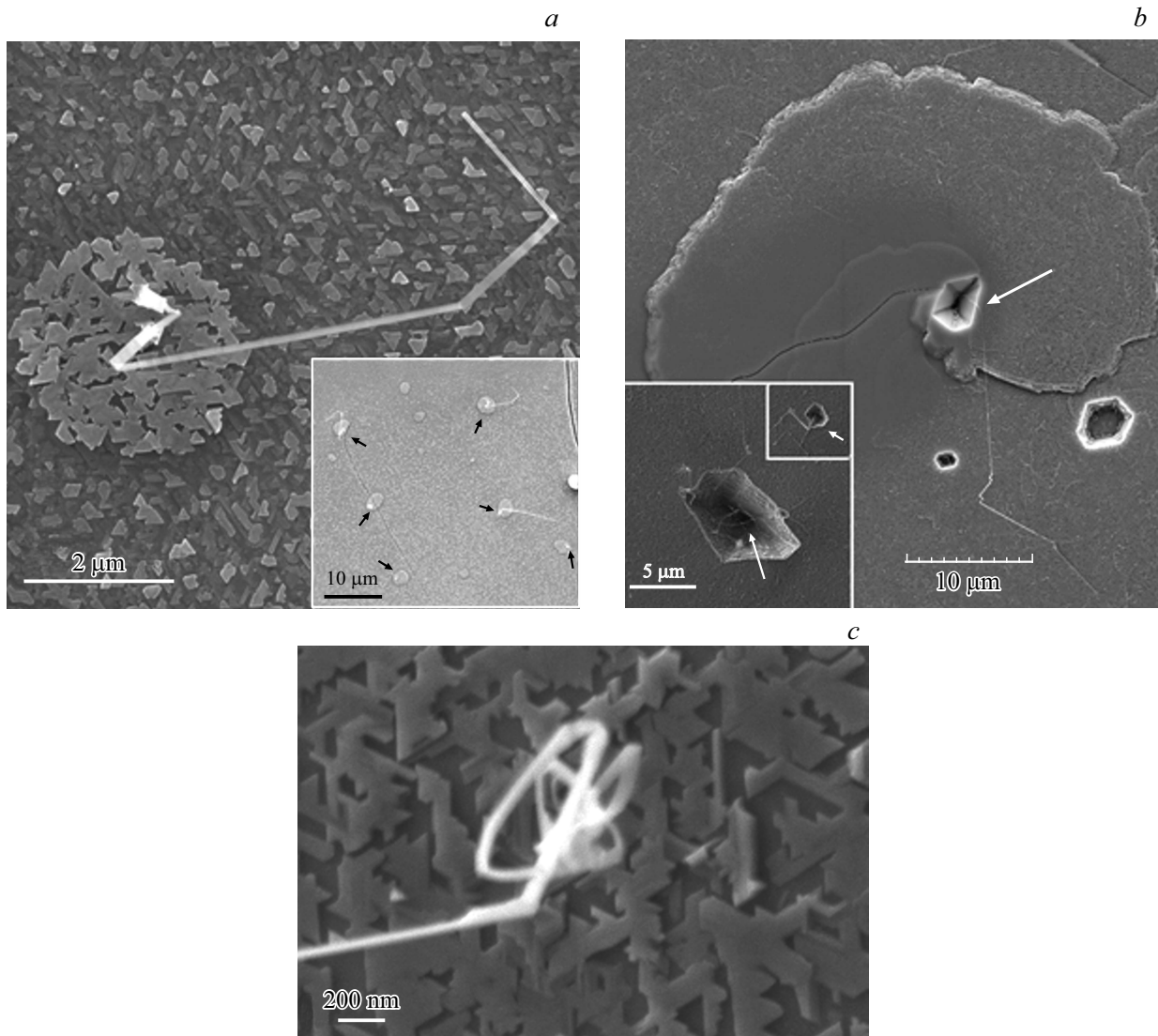


Figure 1. SEM images of growth of whisker nanocrystals on pedestals on the InGaN surface on the substrate with orientation (110) (*a*) and at the dislocation emergence point on the (111) substrate (*b, c*). The inset in panel *a* demonstrates the region with pedestals with a separate nanocrystal growing on each of them. Panel *c* illustrates the initial stage of growth of a „twisted“ WNC.

InN is stretched along axis *c*; i.e., compression is performed along axis *a*. Note that these estimates are fairly rough, since the system contains solid solutions $\text{In}_x\text{Ga}_{1-x}\text{N}$ instead of pure substances. Note also that the signs of σ_{InN} and σ_{GaN} values on the (110) substrate differ. This alters the nature of film growth considerably relative to the case of growth on the (111) substrate.

Figure 1, *b* shows the image of the (111) substrate surface. Ribbon-type WNCs growing from *V*-defects form on it. The process of their formation is similar to the uncoiling of a wrapped hairspring: when set free, its end, which has a certain rotational moment, starts rotating randomly, becomes more and more intertwined, and forms a knot of intertwined whisker nanocrystals. This mechanism is brought into effect by compressive stress and the substantial difference between such stresses in InN and GaN. Being larger than Ga, an In atom on the film surface reacts readily

with HCl and evaporates. It may reside for a short time only in *V*-defects (where almost all stresses are relaxed) and then either evaporates or forms growth layers on the surface of *V*-defect walls. In the course of their „twisting,“ these layers become more and more compressed; this eventually results in their detachment from the walls of *V*-defects and subsequent free growth along the substrate surface. As was demonstrated in [15], the formation of *V*-defects in a GaN layer is associated with the formation of small-angle grain boundaries that induce elastic strain, deviations from the stoichiometric composition of adatoms (from an ensemble of which a GaN film grows), and the formation of a dislocation. Layer-spiral GaN growth [16] later proceeds at this site (this is evidenced by the partially incomplete upper layer), and the WNC nucleation itself occurs in the immediate vicinity or at the core of a dislocation. The average length of ribbon nanocrystals is 30–60 μm. Note

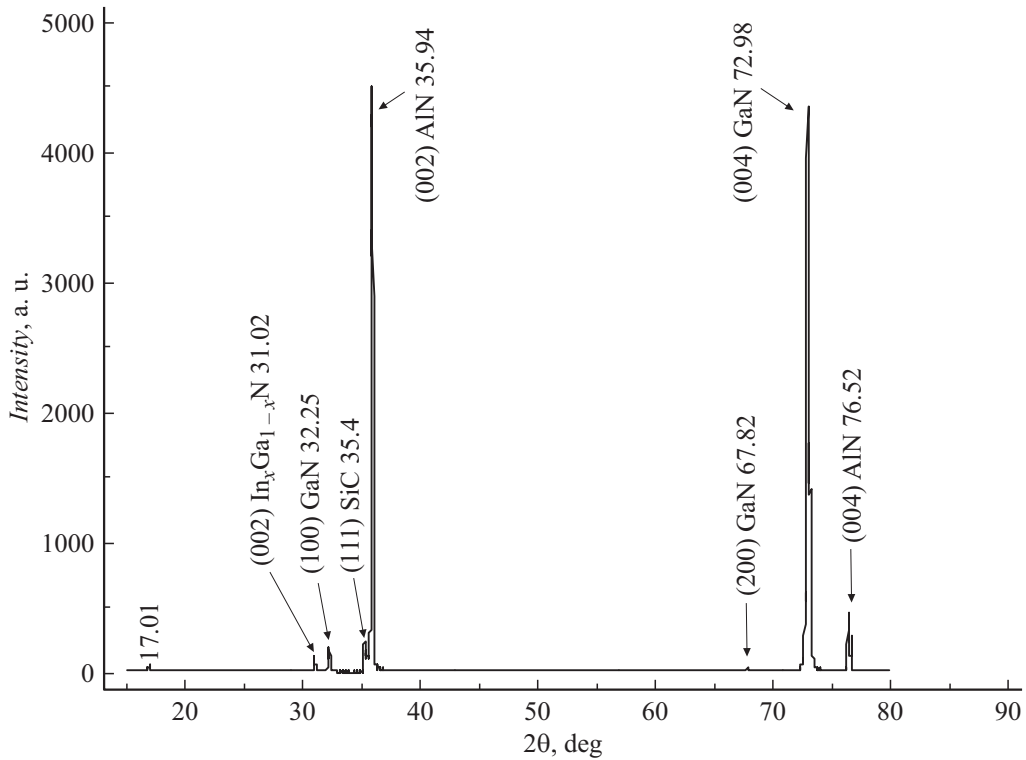


Figure 2. X-ray diffraction pattern of the InGaN sample grown on the SiC/Si (111) substrate.

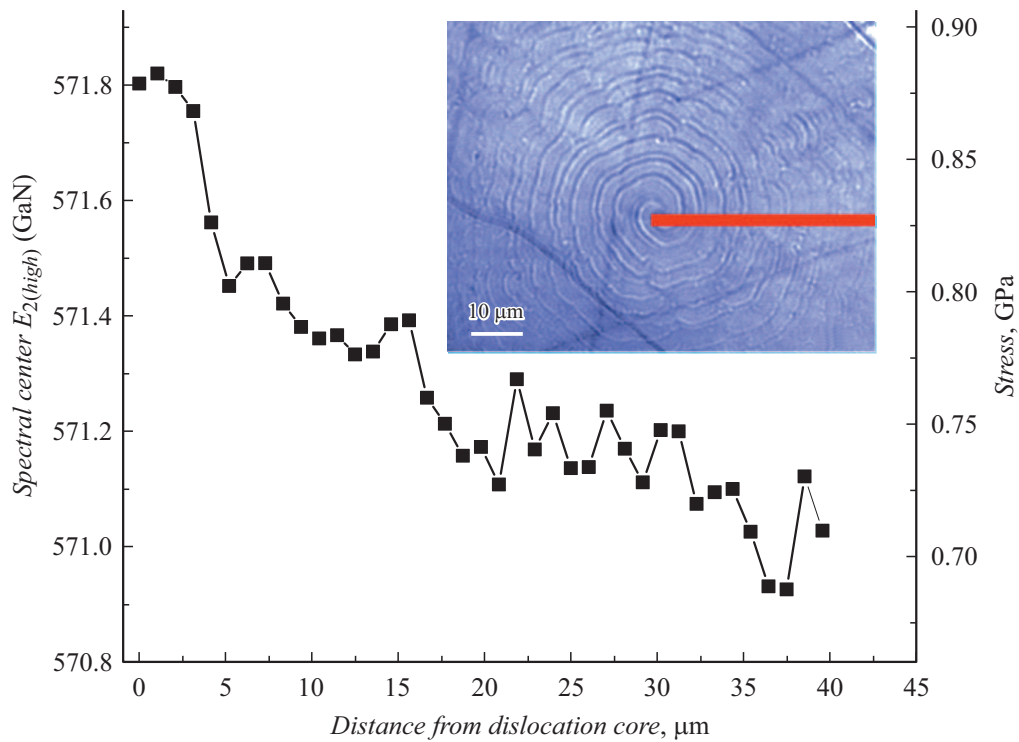


Figure 3. Position of Raman line $E_{2(high)}$ and elastic stresses estimated based on this position at different distances from the dislocation core. Measurements were performed along the line indicated in the inset.

that elastic stresses are maximized near the dislocation core (but outside of it) and relaxes abruptly at the core. A series of Raman spectra of the film were measured at

different distances from the dislocation core to obtain an estimate (Fig. 3). Elastic stresses σ (Fig. 3) were determined using the $\Delta\omega = 4.3\sigma$ [$\text{cm}^{-1}/\text{GPa}$] formula [18] based on

the shift of one of the primary $\text{In}_x\text{Ga}_{1-x}\text{N}$ peaks $E_{2(\text{high})}$ ($\sim 568 \text{ cm}^{-1}$ at $x < 0.05$ [17,18]). Elastic stresses are as high as 0.88 GPa near the dislocation core and decrease to ~ 0.7 GPa outside of the dislocation region. Note that the obtained estimate is also fairly rough [17], since the position of the Raman line also depends on molar fraction x of indium in the solid solution.

Just as on the substrate with orientation (111), ribbon-type WNCs formed on the surface of the (110) substrate (Fig. 1, *a*). However, the case of (110) is different in that WNCs nucleate on the surface of coalesced nuclei of the top GaN layer, which form pedestals. One of the nuclei in a conglomerate (pedestal) serves as the seed for nanocrystals. Note that the growth of WNCs on pedestals was observed in [19], although the size of pedestals was generally comparable to the WNC diameter. In the present case, the diameter of a conglomerate (pedestal) is on the order of $2\text{--}3 \mu\text{m}$ and is thus considerably larger than the WNC diameter. At the initial stage of growth, ribbon WNCs on the (110) surface do not intertwine. They are arranged parallel to the substrate surface and feature long straight sections with kinks of an overall length on the order of $10 \mu\text{m}$. Note that whisker crystals growing in accordance with this mechanism are seen only on pedestals (see the inset of Fig. 1, *a*). If we apply the above reasoning, this mechanism is completely understandable. Averaged within the GaN layer on the (110) surface, elastic stresses are tension-type. The formation of conglomerates (pedestals) is associated with defects in the layer below them. Elastic (tension) stresses induce differences in composition of the vapor phase above a pedestal and above the free substrate surface. Since it is advantageous for large In atoms to adsorb on a pedestal, a WNC nucleates eventually on top of it.

Thus, new mechanisms of WNC growth in HVPE growth of InGaN on *nano*-SiC/Si substrates were implemented in the present study. It was demonstrated that indium added to the vapor phase serves as a catalyst and stimulates WNC nucleation.

Acknowledgments

This study was carried out using the equipment of the unique scientific unit „Physics, Chemistry, and Mechanics of Crystals and Thin Films“ (Institute for Problems in Mechanical Engineering of the Russian Academy of Sciences, St. Petersburg).

The authors would like to thank the TESCAN LLC demo laboratory for assistance in scanning electron microscopy and A.S. Grashchenko for his help in preparing the SiC/Si sample.

Funding

This study was supported financially by the Russian Science Foundation (grant No. 19-72-30004).

Conflict of interest

The authors declare that they have no conflict of interest.

References

- [1] V.O. Gridchin, K.P. Kotlyar, R.R. Reznik, A.S. Dragunova, N.V. Kryzhanovskaya, V.V. Lendyashova, D.A. Kirilenko, I.P. Soshnikov, D.S. Shevchuk, G.G. Cirlin, *Nanotechnology*, **32** (33), 335604 (2021). DOI: 10.1088/1361-6528/ac0027
- [2] E. Roche, Y. Andre, G. Avit, C. Bougerol, D. Castelluci, F. Reveret, G. Evelyne, F. Medard, J. Leymarie, T. Jean, V.G. Dubrovskii, A. Trassoudaine, *Nanotechnology*, **29** (46), 465602 (2018). DOI: 10.1088/1361-6528/aadc1
- [3] H. Hijazi, M. Zeghouane, J. Jridi, E. Gil, D. Castelluci, V.G. Dubrovskii, C. Bougerol, Y. Andre, A. Trassoudaine, *Nanotechnology*, **32** (15), 155601 (2021). DOI: 10.1088/1361-6528/abdb16
- [4] V.O. Gridchin, R.R. Reznik, K.P. Kotlyar, A.S. Dragunova, N.V. Kryzhanovskaya, A.Yu. Serov, S.A. Kukushkin, G.E. Cirlin, *Pis'ma Zh. Tekh. Fiz.*, **47** (21), 32 (2021) (in Russian). DOI: 10.21883/PJTF.2021.21.51626.18894
- [5] Y. Sato, S. Sato, *J. Cryst. Growth*, **144** (1-2), 15 (1994). DOI: 10.1016/0022-0248(94)90004-3
- [6] H. Sunakawa, A. Atsushi Yamaguchi, A. Kimura, A. Usui, *Jpn. J. Appl. Phys.*, **35** (11A), L1395 (1996). DOI: 10.1143/JJAP.35.L1395
- [7] N. Takahashi, J. Ogasawara, A. Koukitu, *J. Cryst. Growth*, **172** (3-4), 298 (1997). DOI: 10.1016/S0022-0248(96)00751-8
- [8] I. Grzegory, S. Krukowski, J. Jun, M. Bockowski, M. Wroblewski, S. Porowski, *AIP Conf. Proc.*, **309** (1), 565 (1994). DOI: 10.1063/1.46099
- [9] K. Hanaoka, H. Murakami, Y. Kumagai, A. Koukitu, *J. Cryst. Growth*, **318** (1), 441 (2011). DOI: 10.1016/j.jcrysgro.2010.11.079
- [10] S.A. Kukushkin, A.V. Osipov, *Pis'ma Zh. Tekh. Fiz.*, **47** (19), 51 (2021) (in Russian). DOI: 10.21883/PJTF.2021.19.51516.18879
- [11] B. Dzuba, T. Nguyen, Y. Cao, R.E. Diaz, M.J. Manfra, O. Malis, *J. Appl. Phys.*, **130** (10), 105702 (2021). DOI: 10.1063/5.0058154
- [12] S.A. Kukushkin, A.V. Osipov, *J. Appl. Phys.*, **113** (2), 024909 (2013). DOI: 10.1063/1.4773343
- [13] S.A. Kukushkin, Sh.Sh. Sharofidinov, *Phys. Solid State*, **61** (12), 2342 (2019). DOI: 10.1134/S1063783419120254
- [14] Sh.Sh. Sharofidinov, S.A. Kukushkin, A.V. Red'kov, A.S. Grashchenko, A.V. Osipov, *Tech. Phys. Lett.*, **45** (7), 711 (2019). DOI: 10.1134/S1063785019070277
- [15] S.A. Kukushkin, Sh.Sh. Sharofidinov, A.V. Osipov, A.V. Red'kov, V.V. Kidalov, A.S. Grashchenko, I.P. Soshnikov, A.F. Dydenchuk, *ECS J. Solid State Sci. Technol.*, **7** (9), P480 (2018). DOI: 10.1149/2.0191809jss
- [16] A.V. Redkov, S.A. Kukushkin, *Cryst. Growth Des.*, **20** (4), 2590 (2020). DOI: 10.1021/acs.cgd.9b01721
- [17] S. Hernández, R. Cuscó, D. Pastor, L. Artús, K.P. O'Donnell, R.W. Martin, I.M. Watson, Y. Nanishi, E. Calleja, *J. Appl. Phys.*, **98** (1), 013511 (2005). DOI: 10.1063/1.1940139
- [18] S. Tripathy, S.J. Chua, P. Chen, Z.L. Miao, *J. Appl. Phys.*, **92** (7), 3503 (2002). DOI: 10.1063/1.1502921
- [19] Y.Y. Hervieu, *J. Cryst. Growth*, **568-569**, 126187 (2021). DOI: 10.1016/j.jcrysgro.2021.126187